Korean J. Chem. Eng., 39(8), 1975-1980 (2022)
DOI: 10.1007/s11814-022-1061-z

pISSN: 0256-1115
eISSN: 1975-7220

Sustainable building materials employing solid diamines as CO_2 sorbents

Suk Lee*, Yun-Ho Ahn,†, and Dong-Yeun Koh***,†**

*Department of Architecture, Kyung Hee University, 1732 Deogyeong-daero, Giheung-gu, Yongin-si, Gyeonggi-do 17104, Korea
**Department of Chemical Engineering, Soongsil University, 369 Sangdo-ro, Dongjak-gu, Seoul 06978, Korea
***Department of Chemical and Biomolecular Engineering, Korea Advanced Institute of Science and Technology,
291 Daehak-ro, Yuseong-gu, Daejeon 34141, Korea

(*Received 9 November 2021 • Revised 23 December 2021 • Accepted 3 January 2022*)

Abstract−The storage of large quantities of CO_2 in a chemically-bonded framework is a key factor in establishing an energy efficient and environmentally sound society. The solvent scrubbing process provides an economically feasible way to capture CO_2 industrially. However, it suffers from inherent problems such as corrosion/leakage problems, difficulty with the regeneration process, and potential environmental issues. In this regard, the solid adsorbent is deemed as a next-generation carbon-capture platform. However, most reported materials involve complex and expensive synthesis processes, hampering their practical use in the field. Inspired by the concept of solid-supported amines and by the reversible sorption of CO_2 in amine solutions, in this paper, we assess the CO_2 sorption performance of raw diamine solid molecule of *p*-phenylenediamine (pPD), which could be coupled with construction materials to meet the design construction standards for sustainable buildings. CO_2 sorption induced structural transformation of pPD and morphology-change induced enhancement of CO_2 sorption kinetics are presented.

Keywords: para-Phenylenediamine, CO_2 Sorbing Materials, Building Materials

INTRODUCTION

Many gigatons of carbon dioxide (CO_2) are annually released into the atmosphere; thus, the development of carbon capture and sequestration (CCS) technologies has become critical to promote environmental sustainability. Among flue gases produced from various industrial processes, CO_2, which exists at low partial pressure, needs to be recycled. In the current portfolio, two different processes are considered as major types of CO_2-capture technology: (1) an alkanolamine solvent-based CO_2 scrubbing (chemical absorption) process based on carbamate formation chemistry (the N-C bonding energies are commonly ~100 kJ/mol) [1], and (2) a porous-material-based physical adsorption process [2,3]. These can compete and complement each other in treating large amounts of CO_2 from flue gases.

Although the alkanolamine solvent CO_2 scrubbing process is economically most feasible, it also has several inherent problems, including a low CO_2 absorption capacity, volatility of the amine solution, difficulty with regard to a regeneration process, corrosion with leakage, and possible environmental issues related to the disposal of the solvent [1]. To resolve those issues, most recent studies have focused on the development of porous materials such as metal-organic frameworks [2,4], mesoporous silica [5,6], and mesoporous carbons and amorphous carbons [7-9] for CO_2 adsorption with high selectivity and affinity. Among porous systems, amine-functionalized solid materials have a low energy cost for the facile regeneration of CO_2 with enhanced CO_2 uptake [10]. Less basic amine groups attached inside the porous frameworks preferentially uptake CO_2 molecules, which significantly reduces the regeneration energy. However, knowledge of the molecular dynamics pertaining to the N-C interaction between the amine and the carbon dioxide remains insufficient [10]. Moreover, most reported materials involve complex and expensive synthesis processes, limiting their practical use in the field. Furthermore, these porous sorbents have a chance to be combined with construction materials that can serve as green building materials. For example, as the effect of CO_2 curing on the properties of concrete has been extensively investigated [11,12], CO_2 sorbing materials can be coupled with cement to develop a practical strategy for the permanent CO_2 sequestration in building materials. The predicted market for building materials combined with waste CO_2 is expected to be further expanded by urging demands for establishing green building and construction materials. Also, there are several design construction standards such as green building rating systems like Leadership in Energy and Environmental Design (LEED) and Building Research Establishment Environmental Assessment Method (BREEAM).

Inspired by the concept of solid-supported amines and the reversible binding of carbon dioxide in amine solutions, we present a selective CO_2 capture method that uses a naturally given solid amine crystal. We suggest the direct use of raw amine crystals, which can efficiently absorb CO_2 at elevated pressures in their native state, without the requirement of a material treatment process such as dissolving in the solvent or grafting the material onto microporous solid supports. As a proof-of-concept, we assessed the CO_2 sorption performance of raw diamine solid particles; para-phenylenediamine (pPD) has two primary amines attached to a benzene ring in the para-position with the chemical formula of $C_6H_4(NH_2)_2$. Para-phenylenediamine has been widely used to tune the CO_2 sorbing materials due to its intrinsic properties of CO_2 capture; various CO_2 sorbing

---

†To whom correspondence should be addressed.
E-mail: yhahn@ssu.ac.kr, dongyeunkoh@kaist.ac.kr

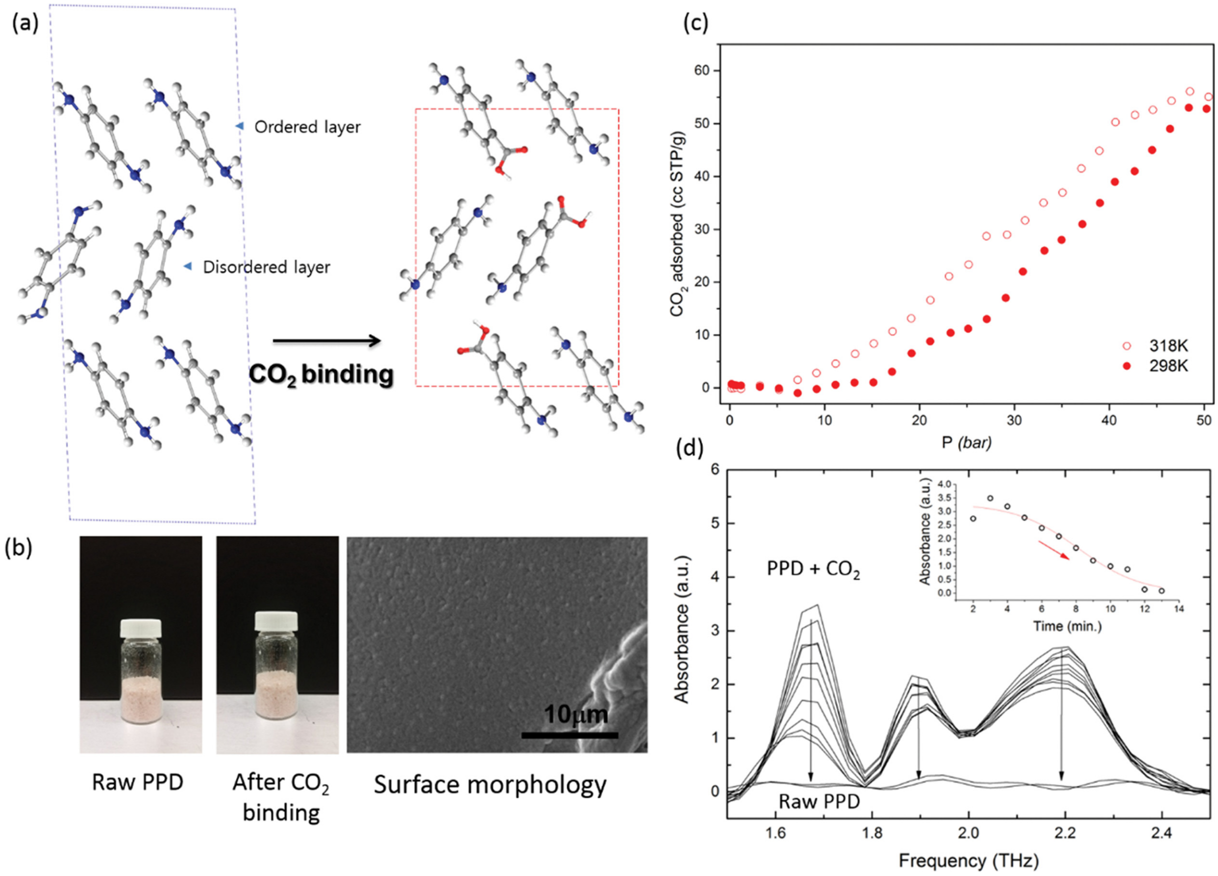

Fig. 1. (a) Schematic illustration of CO$_2$ uptake in pPD crystal structure. (b) Picture of raw pPD, CO$_2$+pPD and SEM micrograph of raw pPD (from the left). (c) High-pressure CO$_2$ isotherm at 298 K (closed circle) and 318 K (open circle). (d) Absorbance spectra measured using THz-TDS at 298 K.

materials such as pPD-modified carbon black [13] or pPD-functionalized microporous organic polymer [14] have been reported. This study focuses on CO$_2$ sorption behavior occurring in raw pPD crystals accompanied by a unique structural/morphological change. Under ambient conditions, pPD has a monoclinic crystal structure with space group P$_{21}$/c (Fig. 1(a), left) [15], showing a purplish color and a plain surface morphology (Fig. 1(b)). pPD is commonly used as a precursor in the fabrication of aramid plastics such as Kevlar. When it is polymerized into aramid plastics, two amines bridge monomers by forming carbamate moieties implying their potential CO$_2$ uptake ability.

MATERIALS AND METHODS

1. Materials

para-Phenylenediamine (pPD) was supplied from Sigma-Aldrich. pPD powders were dried at 353 K overnight before usage. CO$_2$ gas with purity of 99.999% was supplied from Special gas (South Korea). ^{13}CO$_2$ gas with purity of 99% was supplied from Cambridge Isotope Laboratories Inc. (USA).

2. CO$_2$ Sorption and Sample Handling

Low and high-pressure CO$_2$ sorption was measured at 298 K and 318 K up to 760 mmHg using the ASAP 2020 and up to 55 bar using a high-pressure volumetric analyzer (HPVA-100), Micromeritics USA. Samples were dried at 353 K overnight before any CO$_2$ sorption experiments.

A constant-volume pressure-decay reactor was used for kinetics of CO$_2$ sorption in pPD. For every sorption experiment, pPD was used as purchased (unprocessed) simply after drying it overnight under a vacuum at 353 K. Then, ~1 g of pPD powder was placed in a constant-volume pressure-decay reactor and allowed to react with CO$_2$ at room temperature at various pressures. When the steady-state of CO$_2$ sorption was reached, the pressure-decay reactor was rapidly vented, and CO$_2$-loaded pPD powders were collected in liquid nitrogen. This process was done in less than 1 min to minimize unexpected CO$_2$ releasing from pPD powders. CO$_2$-loaded pPD powders were stable in the liquid nitrogen, and no further desorption of CO$_2$ was observed. To explore the effect of the phase of CO$_2$ on the structure of the reaction product, we prepared liquid CO$_2$ (6.7 MPa at 298 K) and injected it into the pPD powder-loaded reactor. As we injected liquid CO$_2$ into the reactor, some remaining CO$_2$ was converted into the solid form when the CO$_2$-loaded pPD powders were transferred to liquid nitrogen. Thus, the formation of solid CO$_2$ is inevitable for this experiment. The samples were directly used for further structural characterization.

3. Characterization

The experimental setup for the fs-THz beamline at the Pohang Accelerator Laboratory is described in detail in the literature [16].

One region of a low-temperature cell and the beam path was surrounded and maintained at a relative humidity of less than 0.5%. Signals were averages of four scans for each measurement; the step size was 30 fs, determined using time-domain spectroscopy. A proper amount of the CO_2-loaded pPD powders was placed between the pre-cooled THz-grade crystal quartz (~80 K), and the quartz windows were loaded in the copper cell, which was fixed in a variable-temperature cell holder. The sample spectrum was measured at 80 K, and the temperature was gradually increased up to 298 K.

A Varian (UnityNOVA600) 600 MHz solid-state NMR spectrometer was employed to examine the chemically bound CO_2 to pPD. The finely ground (≈200 μm) powdered samples were loaded into a ZrO_2 rotor (2 mm outer diameter) under liquid nitrogen, and then a rotor was quickly transferred into a variable temperature probe. All ^{13}C NMR spectra were recorded at a Larmor frequency of 100.6 MHz with a magic angle spinning at about 10 kHz, and the measurement temperature was fixed at 183 K.

The HRPD patterns were collected using the Pohang Accelerator Laboratory (PAL) synchrotron. During the measurements, the $\theta/2\theta$ scan mode with a fixed time of 2 s and a step size of 0.005° for 2θ=0-120°, and the beamline with a wavelength of 1.5472 Å were used for each sample. The samples were loaded at 77 K to minimize the possible CO_2 desorption.

RESULTS AND DISCUSSION

High-pressure CO_2 isotherms of the pPD crystal were measured at 298 K and 318 K, as shown in Fig. 1(c). In a low-pressure regime (<10 bar), the interaction between CO_2 and pPD is very weak, presumably due to the lack of micropores in pPD, providing a considerable barrier to CO_2 diffusion into materials. When the pressure is increased until it exceeds 10 bar, CO_2 uptake increases gradually with an increase in the pressure, similar to the unpreferred adsorption isotherm. Total CO_2 sorption reaches 52 cm^3/g (2.31 mmol/g) at 298 K, and the uptake increases to 56 cm^3/g (2.45 mmol/g) at 318 K. Fig. 1(b) compares the pPD powders before and after CO_2 uptake, showing a marginal change in the color and powder size.

We found that CO_2 desorption occurred at room temperature under atmospheric pressure, and the material fully recovered to its original structure within 30-40 minutes. As spectroscopic evidence of the CO_2 desorption from pPD structure, Fig. 1(d) represents the terahertz time-domain spectra (THz-TDS) during desorption of CO_2 from pPD at 298 K and atmospheric pressure. CO_2-loaded pPD particles were loaded to the in-situ cell at 77 K. The measurement began when the temperature of the in-situ cell reached 298 K (heating rate=5 K/min). The distinct absorbance peaks at 1.7, 1.9, and 2.2 THz originating from incorporated CO_2 in the pPD structure gradually decreased as CO_2 was desorbed from the pPD. This proves that when the CO_2 pressure is not present, pPD releases CO_2 molecules even at mild pressure and temperature conditions. Within 20 minutes, the spectrum turned to its original spectrum of raw pPD. The gradual decrease in the absorbance at 1.7 THz is shown in the inset. This facile regeneration characteristic of pPD can enhance the CO_2 curing rate if it is added to the cement mixture; released CO_2 from pPD at a molecular level can efficiently react with calcium hydroxide eliminating a slow CO_2 diffusion through the bulk cement phase.

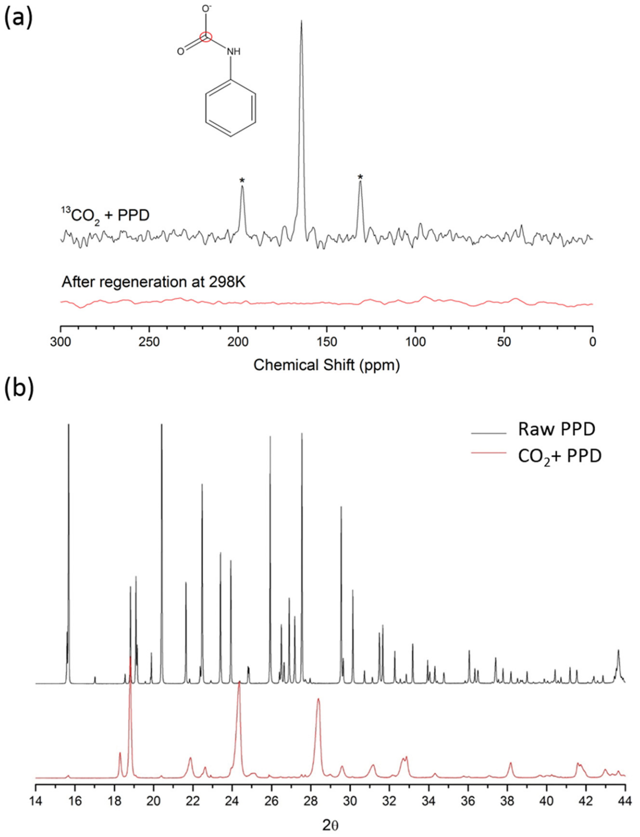

Fig. 2. **(a) Solid-state ^{13}C NMR (CP/MAS) spectra measured at 183 K. $^{13}CO_2$+pPD (black) and same sample regenerated at 298 K (red). Asterisk indicates spinning sideband. (b) Synchrotron HRPD patterns of raw pPD (black) and CO_2+pPD (red).**

To obtain chemical and structural details of the CO_2-loaded pPD, we measured the ^{13}C solid-state NMR and synchrotron high-resolution x-ray powder diffraction (HRPD) patterns. ^{13}C-labeled CO_2 was used in the reaction with pPD, and the $^{13}CO_2$-loaded sample was transferred to liquid nitrogen to prevent any CO_2 desorption. CP/MAS ^{13}C NMR spectra of the CO_2-loaded pPD recorded at 183 K show a single peak at 164.1 ppm, as shown in Fig. 2(a), which indicates that CO_2 is covalently bound to pPD through the formation of a carbamate group between the CO_2 and the amine of pPD. Moreover, Fig. 2(b) shows HRPD patterns of the raw pPD and the 'CO_2+pPD' measured at 80 K (ex-situ HRPD experiments were conducted at the 9B beamline of the Pohang Accelerator Laboratory (PAL) in South Korea). HRPD pattern of the raw pPD is fitted with the space group of P_{12}/c (a=8.2935, b=5.8877, and c=22.7199), as reported in earlier work [15]. When pPD reacts with CO_2, the HRPD pattern shows a high angle shift of the lowest 2θ peak and a decrease in the overall number of reflection peaks (17 new peaks emerged within the 2θ range of 10 to 35°). This implies that the CO_2-induced phase transition drastically changes the structure by shrinking the unit cell of pPD and yielding a more symmetric structure when CO_2 is loaded intramolecular position. Plausible CO_2+pPD structure has an orthorhombic P_{21}/m space group hav-

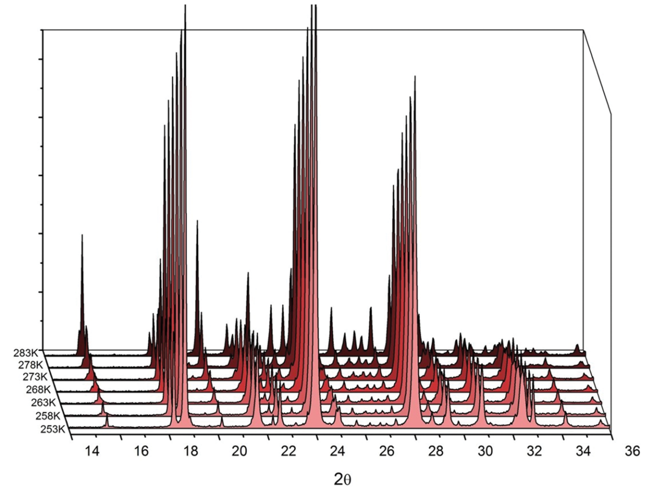

Fig. 3. HRPD pattern of CO_2+pPD recorded by heating the sample from 253 K to 283 K. Gradual changes in the pattern indicate the CO_2 desorption induced structure change.

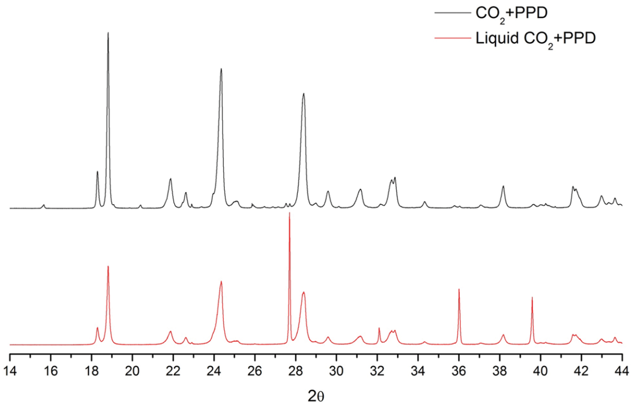

Fig. 4. HRPD pattern of liquid CO_2+pPD. Sharp peak at 27, 32, 36 and 39° is dry ice impurity. Marginal difference between gas phase reaction and liquid phase reaction is observed.

ing; 1) unique range b-axis that is similar to that of the raw pPD structure (b=5.88 Å vs. 6.12 Å), and 2) an elongated c-axis which explains the CO_2 storage in the interlayer between ordered layers (c=22.76 Å vs. 12.59 Å). We note that analogous structural transition behavior was previously reported; raw pPD with a monoclinic structure was transformed into orthorhombic pPD-2H_2O upon water adsorption to pPD [17]. In this case, the atomistic origin of the phase transformation into the higher symmetric phase is discussed as a transition of the disordered layer of pPD into an ordered layer while the pPD-H_2O interaction develops. In addition, hydrogen bonding between pPD and H_2O induces elongation of the c-axis while maintaining the unique axis of the b-axis. We thus expect that a similar mechanism was involved in the structural transition induced by CO_2 uptake in the pPD.

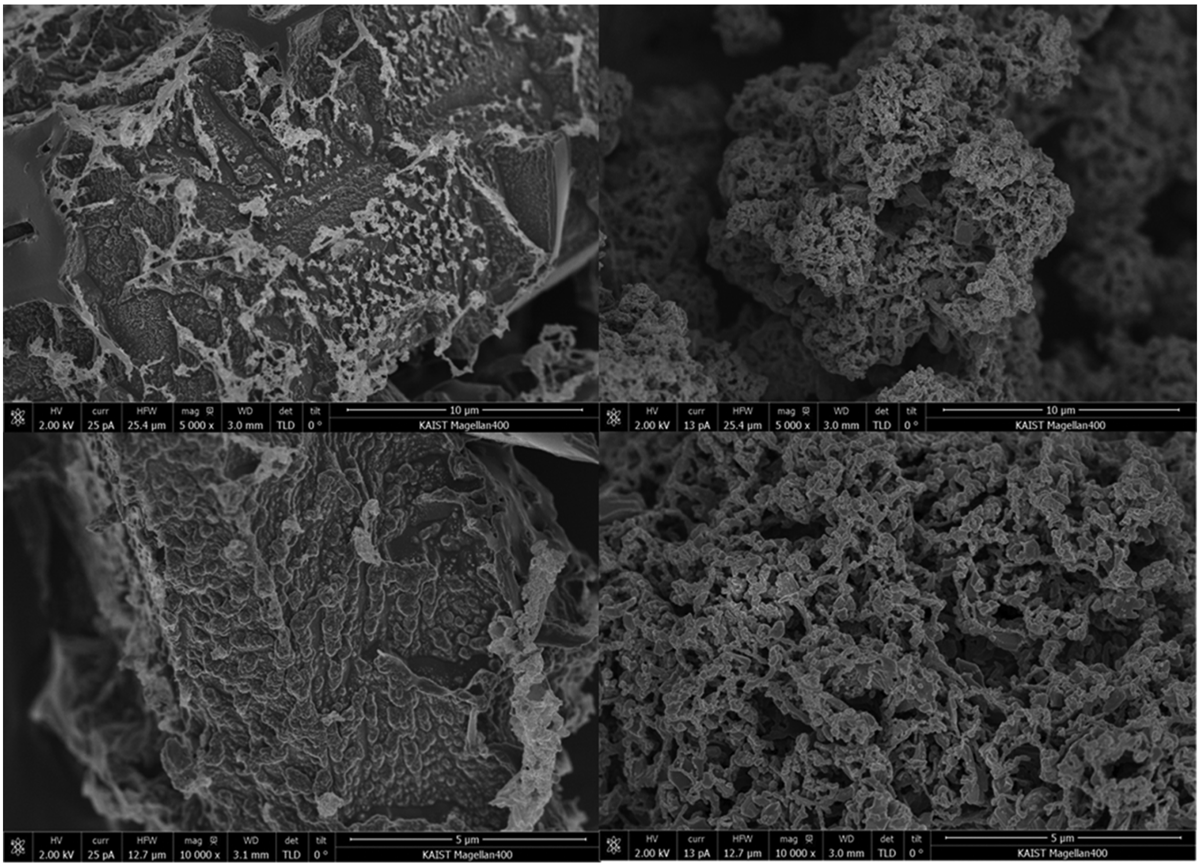

Fig. 5. SEM micrographs of unreacted pPD (left) and CO_2 desorbed pPD (right).

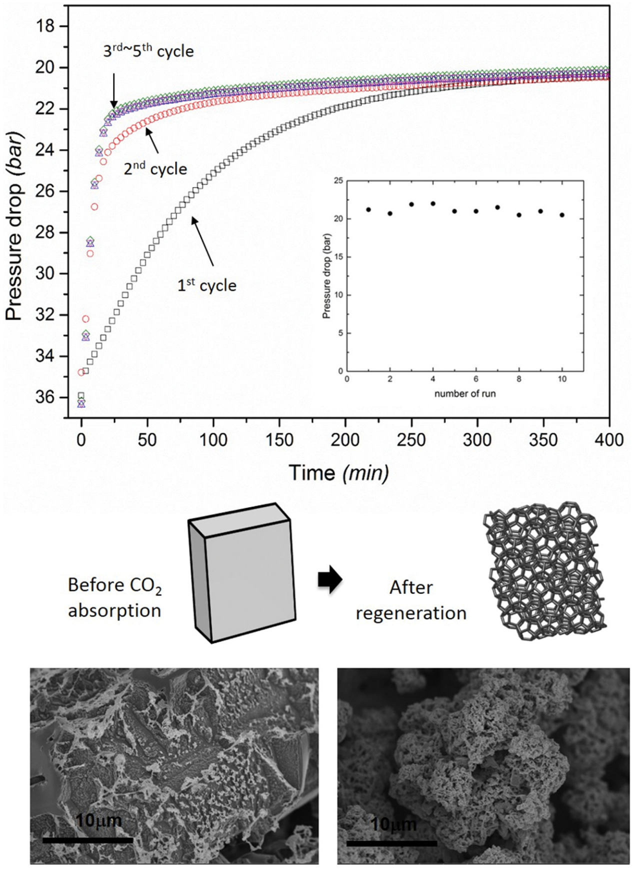

Fig. 6. CO_2 uptake/desorption kinetics at 298 K. Inset graph shows the constant CO_2 uptake amount obtained up to ten sorption/desorption cycles.

Using HRPD, we studied the structural transition during CO_2 desorption more closely by heating the sample stage to 283 K (Fig. 3). Starting at 253 K, it was found that CO_2 desorption occurs, as evident from the change in the intensity of the peaks, as the HRPD sample stage uses a high vacuum. When the temperature reaches 283 K, most of the reflection peaks are recovered to those of the original pPD, indicating that the sorption-desorption process is fully reversible and that the original crystal structure is recovered and regenerated. However, as shown in Fig. 1(b) and Fig. 6, the surface morphology of the powder is drastically modified when a full cycle of CO_2 sorption and desorption is finished. Additional SEM images are shown in Fig. 5. As discussed above, although the raw pPD crystal before the adsorption of CO_2 shows a plain crystalline surface (Fig. 1(b), lower left), macro-pores were generated after one CO_2 adsorption-and-desorption cycle. We further tested with liquid CO_2 to react with pPD and compared the structure using HRPD (Fig. 4). Except for dry ice impurities formed during the sample handling process [18], the HRPD pattern of liquid CO_2-loaded pPD and gaseous CO_2-loaded pPD shows the marginal difference.

The development of such a porous morphology allows the more rapid diffusion of gaseous CO_2 molecules (additional SEM images in Fig. 5), which is beneficial for enhancing the CO_2 sorption kinetics for further cycles. Indeed, the cyclic CO_2 uptake experiment shown in Fig. 6 clearly indicates the kinetic enhancement effect induced by the macro-morphological change. Each sorption-desorption experiment was performed using a single constant-volume reactor, and the decay in the pressure by CO_2 uptake in the pPD was recorded. When the fresh (dried) pPD powder was loaded into the reactor, and pressurized CO_2 was supplied (first cycle), the tail of the pressure decay curve was elongated up to 250 minutes of the reaction, and a plateau was obtained. Once regenerated at room temperature and atmospheric pressure (second cycle), the same amount of CO_2 was re-injected into the reactor, after which it was observed that the CO_2 sorption kinetics was greatly improved. CO_2 sorption that was nearly twice as fast was achieved up to 50 minutes in the second cycle. The CO_2 sorption kinetics was further increased in the third cycle, and similar sorption trends were observed after the third run. Therefore, it is concluded that the massive and rapid desorption of CO_2 during the regeneration step creates macropores in the crystalline pPD structure, through which CO_2 diffuses rapidly. Thus, the sorption kinetics is enhanced after one or two cycles. It was also noted that the increase in the BET surface area (from 0.22 m^2/g to 12.11 m^2/g) before and after the first cycle supports the formation of a macro-porous structure (Fig. 7).

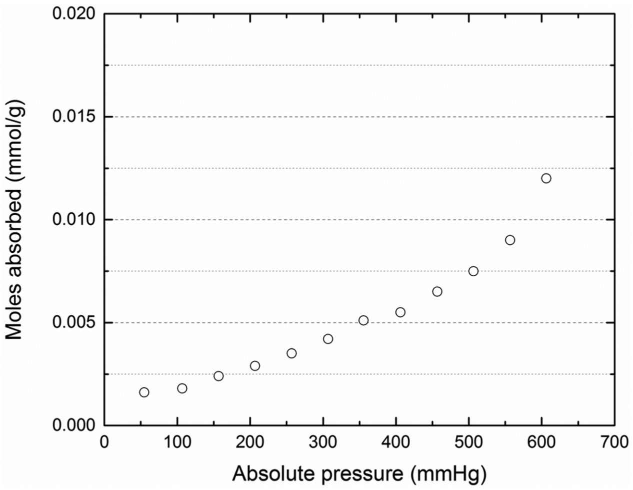

Fig. 7. N_2 adsorption isotherm of pPD after CO_2 desorption recorded at 77 K. BET surface area is calculated to 12.11 m^2/g.

Although the CO_2 uptake kinetics is improved as the cycle increases, each cycle shows similar equilibrium uptake amounts and pressure drop values (Δp) for ten consecutive runs, as shown in the inset of Fig. 4. This indicates that the underlying chemistry of CO_2 adsorption to pPD is maintained throughout the cycles.

CONCLUSIONS

We have presented the use of a raw (un-processed) crystalline amine compound as a promising and straightforward candidate as a solid CO_2 scrubbing material or an additive for green building material. The attractive features of pPD as a CO_2-capturing material can be summarized as follows. First, pPD can be used as-purchased without any further chemical treatment or synthesis, which is an important benefit from an economic viewpoint with regard to its immediate application in the field. Second, regeneration can be achieved in an ambient condition because pPD easily desorbs CO_2 at room temperature and under atmospheric pressure. Third, the structural change due to the CO_2 uptake process is reversible. Fourth, the gas uptake kinetics is enhanced after a few adsorption-desorption cycles due to the change in the crystal surface morphology. Furthermore, it is possible to use pPD in a natural gas sweetening process because it takes up CO_2 under relatively high-pressure conditions. We anticipate that the solutions in the commonly used solution-driven processes can be replaced with the relatively beneficial solid absorber material of pPD. However, several properties of pPD still require improvement before the practical use of pPD as a CO_2-capturing material can be realized operated under the harsh conditions of flue gas. For instance, we expect that the CO_2 uptake pressure or kinetics can be tuned even further by tailoring the microporosity inside the pPD crystals. More structural optimization steps and the proper design of pPD will offer new insights into the behavior of solid amine materials toward efficient and cost-effective CO_2-capturing technologies.

ACKNOWLEDGEMENTS

This work was supported by the National Research Foundation of Korea(NRF) grant funded by the Korea government (MSIT) (No. 2021R1C1C1012014, 2021R1F1A1047108). It was also supported by Basic Science Research Program through the National Research Foundation of Korea (NRF) funded by the Ministry of Education (No. 2020R1G1A1102678).

FINANCIAL DISCLOSURE

Authors have no relevant financial interests in this manuscript.

REFERENCES

1. J. C. Abanades, E. S. Rubin and E. J. Anthony, *Ind. Eng. Chem. Res.*, **43**, 3462 (2004).
2. B. Wang, A. P. Côté, H. Furukawa, M. O'Keeffe and O. M. Yaghi, *Nature*, **453**, 207 (2008).
3. H. Furukawa and O. M. Yaghi, *J. Am. Chem. Soc.*, **131**, 8875 (2009).
4. M. B. Yue, Y. Chun, Y. Cao, X. Dong and J. H. Zhu, *Adv. Funct. Mater.*, **16**, 1717 (2006).
5. C. Chen, S. T. Yang, W. S. Ahn and R. Ryoo, *Chem. Commun.*, **24**, 3627 (2009).
6. Y. Lee, D. Liu, D. Seoung, Z. Liu, C. Kao and T. Vogt, *J. Am. Chem. Soc.*, **133**, 1674 (2011).
7. A. Wahby, J. M. Ramos-Fernández, M. Martínez-Escandell, A. Sepúlveda-Escribano, J. Silvestre-Albero and F. Rodríguez-Reinoso, *ChemSusChem*, **3**, 974 (2010).
8. G. P. Hao, W. C. Li, D. Qian, G. H. Wang, W. P. Zhang, T. Zhang, A. Q. Wang, F. Schüth, H. J. Bongard and A. H. Lu, *J. Am. Chem. Soc.*, **133**, 11378 (2011).
9. V. Presser, J. McDonough, S. H. Yeon and Y. Gogotsi, *Energy Environ. Sci.*, **4**, 3059 (2011).
10. K. Sumida, D. L. Rogow, J. A. Mason, T. M. McDonald, E. D. Bloch, Z. R. Herm, T. H. Bae and J. R. Long, *Chem. Rev.*, **112**, 724 (2012).
11. T. Wang, H. Huang, X. T. Hu, M. X. Fang, Z. Y. Luo and R. N. Guo, *Chem. Eng. J.*, **323**, 320 (2017).
12. C. Shi and Y. Wu, *Resour. Conserv. Recycl.*, **52**, 1087 (2008).
13. A. Grondein and D. Bélanger, *Fuel*, **90**, 2684 (2011).
14. V. M. Suresh, S. Bonakala, H. S. Atreya, S. Balasubramanian and T. K. Maji, *Acs Appl. Mater. Inter.*, **6**, 4630 (2014).
15. M. Colapietro, A. Domenciano, G. Portalone, G. Schultz and I. Hargittai, *J. Phys. Chem.*, **91**, 1728 (1987).
16. H. Kang, D. Y. Koh, Y. H. Ahn, S. Jung, J. Park, J. Lee and H. Lee, *J. Chem. Eng. Data*, **60**, 238 (2015).
17. A. Czapik, H. Konowalska and M. Gdaniec, *Acta Cryst.*, **C66**, 128 (2010).
18. S. Moon, Y. H. Ahn, H. Kim, S. Hong, D. Y. Koh and Y. Park, *Chem. Eng. J.*, **330**, 890 (2017).